Study of Ion Charging Effect to Improve Reactive-Ion-Etching Profile of PbSe Grating Structures

Tehere Hemati^a, Gang Yang^b and Binbin Weng^{a,b}

^aSchool of Electrical and Computer Engineering, University of Oklahoma, , Norman, 73019, OK, USA

ARTICLE INFO

Keywords: Reactive Ion Etching Charging Effect Lead Selenide Ion-Focusing Bowing Effect

ABSTRACT

This research studies the impact of the charging effect on the RIE-etched profile of narrow-slot Lead-Selenide (PbSe) gratings. By decreasing the slot width from 4 to 2 μm , we observed the increased irregularity and RIE-lag in etched profiles. We suggest that the charging effect is the main responsible mechanism for this phenomenon. The accumulated charge on the non-conductive photoresist plays a crucial role in forming this effect. Therefore, introducing a conductive layer can neutralize the accumulated charge and significantly improves the profile. To prove this theory, we introduced a thin layer of copper on the gratings. While without any conductive coating, we failed to etch gratings with a slot width of less than 1 μm , by introducing a copper layer, we succeeded etching gratings with 0.7 μm slot width with the improved sidewall profiles. Hence, this technique enables us to fabricate sub-micron PbSe gratings with applications of mid-infrared (MIR) devices.

1. Introduction

The mid-infrared (MIR) optical region has significant importance in a broad range of applications, including thermal imaging, remote detection, medical diagnosis, failure analyses, and gas sensing [1, 2, 3, 4, 5, 6, 7]. Controlling light-matter interaction plays an essential role in improving the performance of thin film MIR photonic/optoelectronic devices. [8, 9, 10]. Especially in emerging technologies such as the Internet of Things (IoT), this role becomes more vital in micro-size structures [11, 12]. However, these micro-structures are highly sensitive to size modulation. Thus, a precise fabrication process is essential to achieve the exact size.

To fabricate such micro-structures, the desired pattern is transferred to the substrate by different lithography methods, depending on the pattern resolution. Then, the unwanted parts are removed through an etching process, and the pattern is formed. One of the well-known etching methods is wet chemical etching. This low-cost and straightforward method provides high levels of mask selectivity [13, 14]. However, the equal etched rate in all directions, or in other words, isotropic etching, results in severe undercutting of the masking layer and makes size control challenging [15]. This issue becomes bold in micro-size components, in which high feature size control is needed. In comparison to wetetching, reactive ion etching (RIE) and inductively coupled plasma-RIE (ICP-RIE) indicate high material selectivity and directionality [16, 17] simultaneously. Therefore, this method can be a promising candidate for the fabrication of small-size components with close pitch and high-density arrays. To achieve a precise etching profile with smooth sidewalls, optimizing the plasma gas phase, RIE power, and chamber pressure are significantly important.

binbinweng@ou.edu (B. Weng)
ORCID(s):

IV-VI lead chalcogenide semiconductors (e.g., PbSe, PbTe etc.) have unique material properties, including a broad size-tunability of the bandgap [18], a large Bohr radius and quantum confinement [19], and low Auger recombination coefficients [20], can be a suitable choice for developing MIR optoelectronic devices[21]. However, compared to semiconductors of groups II-VI [22], and III-V [23], and despite the high potential of group IV-VI materials in the fabrication of MIR devices, only a few works have explored RIE etching of IV-VI materials [24]. In recent, we reported an effort to develop a suitable recipe to etch PbSe thin films by the RIE method [6]. However, this work mainly focused on studying the influence of gas stoichiometry on etching performance over the PbSe films, which has yet to study the etching profile over narrow-slot micro-size gratings, which are critical structures for enhancing novel light-matter interaction in the MIR range to improve corresponding devices performance.

In this work, we found out that the previously developed etching recipe results in an unexpected profile irregularity and RIE-lag for sub-micron narrow-gap grating structures. We anticipate that the source of this irregularity can be the charging effect induced by charged carrier shading. Charged carrier shading is a phenomenon that explains the imbalance of ion and electron currents reaching the bottom of the narrow gap [15]. It seems that the accumulated charge on the insulating photoresist builds up a positive charge at the neck of the trench, leading to the deflection of ions and causing a lower etch rate at the trench bottom. To test our hypothesis, we deposited a metallic layer on non-conductive photoresist mask layers to assist in preserving the electrical continuity in intermediate parts and prevent charging up the photoresist, resulting in a minimal shading effect.

^bMicrofabrication Research and Education Center, University of Oklahoma, , Norman, 73019, OK, USA

2. Experimental Details

In this research, we designed a set of grating structures with different slot sizes to study the effect of the gap width. For etching grating patterns, we used PbSe thin films with a thickness of 1 μm , depositing with oriented attachment (OA) chemical solution method on glass substrates. The details of the growing process have been explained in our previous research [21]. Before applying the photoresist, we ultrasonic cleaned the sample in acetone for three minutes, followed by a three-minute ultrasonic clean in Isopropanol alcohol (IPA), and finished by rinsing the sample in deionized (DI) water and drying the sample using ultra high purity (UHP) nitrogen gas. Then, we coated the sample with HMDS to improve photoresist adhesion. Afterward, we spin-coated the sample with AZ nLOF2020, resulting in 2 µm thick photoresist. Then, we soft-baked the sample for one minute at 110 C°. We used the MJB3 mask aligner to transfer the grating patterns to the sample. After four-second UV exposure, we baked the sample again for one minute at 110 C°. Finally, we developed it in AZ 300MIF developer for 50 seconds, washed it with DI water, and dried it using UHP nitrogen gas.

In this study, we used the Trion ICP-RIE plasma etching system (Trion Technology). The reactor chamber was pumped down to less than 1.5×10^{-5} Torr. The RIE was performed in CH₄/H₂/Ar plasma atmosphere, where the gas flow rate was controlled by mass flow controllers [6]. After completing the etching process, the structure was exposed to Oxygen for 240 seconds to improve photoresist removal. After finishing the etching process, to completely remove the photoresists, we ultrasonic the sample in acetone and IPA for three minutes, respectively, and finished by rinsing the sample in DI water and drying it with UHP nitrogen gas.

We used Lesker Nano36 Evaporator to grow a thin copper layer. This system is a 150 W three-source thermal evaporation system, typically used to evaporate metal films under high vacuum (6×10^{-6} Torr) while measuring the thickness in-situ by a thickness monitor. This fully automatic system can completely control the metallization process. After completing the metallization, to remove Cu from unwanted areas, we lifted off the gratings in AZ NMP Rinse for 20 minutes and cleaned them with DI water, and dried them with nitrogen gas.

We characterized the etched structures by scanning electron microscope (SEM) JSM-6060 (JEOL). The top and tilted view SEM images give a comprehensive understanding of the RIE process. Moreover, we used Keyence VHX-7000 digital microscope to provide a 2D profilometer analysis from the etched grating profile.

3. Results and Discussion

Figure 1.(a) shows the SEM photo of the etched profile of a PbSe grating with a period of 8 μm and 50% fill factor. As we can see, the open area where no grating has been patterned and slots in the grating area have been entirely etched to the substrate. The inset shows a 2D profilometer

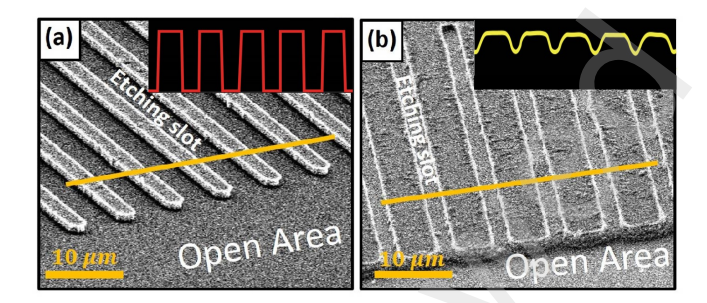


Figure 1: (a) The tilted SEM image of the etched profile of a grating with a slot width of 4 μ m. The inset shows a 2D profilometry view of this grating. (b) The tilted SEM image of the etched profile of a grating with a slot width of 2.1 μ m. The inset shows a 2D profilometry view of this grating. The reference line is displayed by a solid yellow line at the grating area.

analysis given by Keyence VHX-7000. The reference line is displayed by a solid yellow line at the grating area. Figure 1.(b) displays the SEM photo of a grating with a period of 7 μm and 70% fill factor, where the slot width has been reduced from 4 μm to 2.1 μm , compared to the figure 1.(a). While the open area has been etched to the substrate, slots at the grating area show the RIE-lag, and the etching process has not been completed in this area. The 2D profilometer displayed in the inset shows a severe bowing effect in the narrow-slot grating.

Since the main difference between these two gratings is their slot width, we anticipate this factor plays an important role in causing the RIE-lag and the bowing effect. To test this theory, we studied the slot width impact by etching gratings with different slot sizes. We started from a grating with the slot of 4.1 μ m and decreased the slot width 100 nm for each grating. Therefore we provided a set of gratings with the widest slot of 4.1 μ m and the narrowest of 0.7 μ m. All gratings were etched at CH₄/H₂/Ar atmosphere with the ratio

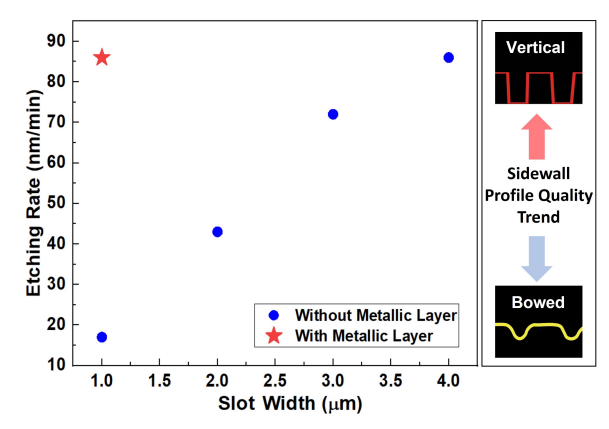


Figure 2: The plot of the etching rate according to slot width changes in grating structures. The blue circles are related to the grating with no metallic layer. The red star shows the accelerated etching rate due to the introduced metallic layer (Cu) for narrow-slot gratings. The arrows show that by increasing the etching rate, the etch profile improves.

of 10/10/5, respectively for 700 s. We found out the bowing effect starts to be noticeable in the grating with the slot of 3 μ m, and for less than 1.5 μ m slot width, the grating pattern severely disordered and etching the grating with less than 1 μ m slot width is practically impossible.

Figure 2 can give us a better understanding of the relationship between slot width and the etching rate in grating structures. The blue circles indicate the etching rate of PbSe gratings, where only insulator photoresists are used for patterning. This plot shows that by increasing the slot width from 1 μ m to 4 μ m, the etching rate increases almost linearly from 17 nm/min to 86 nm/min, and the etched profile improves, resulting in an ignorable bowing effect for gratings with a slot width of 4 μ m.

The source of this irregularity can be the charging effect induced by charged carrier shading. Charged carrier shading is a phenomenon that explains the imbalance of ion and electron currents reaching the bottom of the narrow gap. The primary reason for this phenomenon is related to the difference in the ion and electron angular distributions. When the pattern is exposed to a plasma, the upper side of the mask is charged up. Thus, the entering electrons are deflected, resulting in the reduction of the reaching electron to the bottom of the gap. In addition to profile irregularity, the shading effect can cause the RIE-lag. Ion deflection or translational energy reduction decreases the etch rate at the bottom of the slot.

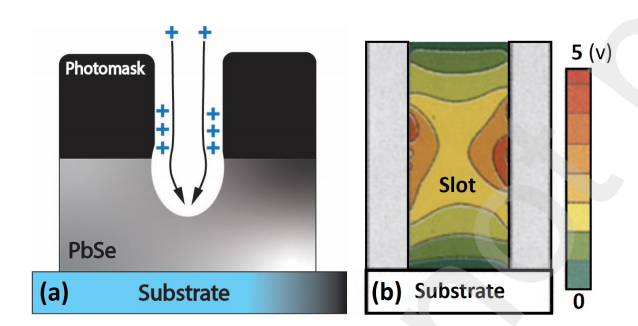


Figure 3: (a) A 2D schematical view of the etched profile of a PbSe grating showing the ion-focusing effect resulting in the rounded shape of the trench's bottom. (b) The numerical simulation of the potential contour map in the slot in a grating. The colored bar shows the potential values of the counter map [15].

As a result of the accumulated electrons on the mask, an intense electric field builds up at the edge gap in the direction of the edge line. These electrons can no longer be distributed to intermediate lines to maintain electrical continuity. Therefore, ions are mostly deflected along the edge line, etching the inner sidewall much sooner than the sidewalls of intermediate lines. This results in etching the open area faster than compacted arrays. This phenomenon mostly leads to micro trenching. However, in this study, the profilometer analysis (figure 1.(b)) indicates the bowing

effect rather than the trenching effect. Although this phenomenon can be the responsible mechanism for the RIE-lag (etching the open area faster than the grating area), it seems that another mechanism is involved leading to the bowing effect. This mechanism can be ion-focusing. The ion-focusing mechanism can be responsible for the rounded shape of the trench bottom. Figure 3 can give us a better understanding of this mechanism.

Figure 3.(a) illustrates a 2D schematical view of the etched profile of a PbSe grating showing the bowing effect. Arrows display ion current trajectory, and positive signs stand for the positively charged area. Figure 3.(b) shows the simulated potential contour map of the slot in a grating [15]. The colored bar shows the potential values of the counter map where the red color is the most positively charged part and the dark green is the neutral part. As we can see, the positive accumulated charge on the trench's sidewall repels the ion current and forces a significant fraction of the ions to bend toward the center of the trench. The schematical view indicates evidently how the ion-focusing results in the rounded bottom, while no indication of trenching is observed. The performed numerical simulation shows how the sidewalls charged up positively (red parts show the highest positive potential).

Since the responsible mechanism for RIE-lag is accumulated charge on the photoresist, it seems that introducing a metallic layer can address this issue. The metallic layer helps to preserve the electrical continuity in intermediate parts and prevents charging up the photoresist and its consequent phenomena. We anticipate that introducing a thin metallic layer can significantly improve the etched profile in a way that fabrication of gratings with a slot width of less than 1 μ m would be possible. To test this theory, we deposited a 70 nm thick copper (Cu) layer on the patterned gratings. In this study, we selected copper due to its decent electrical conductivity, straightforward deposition method, and relatively easy etching removal.

Figure 4.(a) displays the SEM image of the etched grating without the Cu layer. Figure 4 (b) demonstrates the SEM image of the etched grating by introducing a 70 nm Cu layer on the photoresist. Insets show a zoomed-in view of each

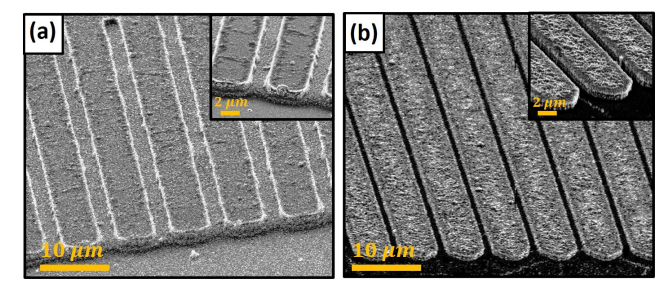


Figure 4: (a) The tilted SEM image of the etched profile of the grating without a Cu layer. The inset shows a zoomed-in view. (b) The tilted SEM image of the etched profile of the grating with 70 nm of Cu layer. The inset shows a zoomed-in view.

grating. The solid yellow bar shows the scales. The gratings have been etched for 700 seconds, at a process pressure of 15 mTorr, 150 watts of RIE power, with a gas mixture of $10CH_a/10H_2/5Ar$.

We can see that without applying any Cu layer (Figure 4.(a)), the etching process of the grating with a slot width of 2.1 μ m and the period of 7 μ m has not been completed. While the open area has been entirely etched, due to the RIE-lag and the ion-focusing effect, the slots have not been etched completely. In comparison, by precisely the same etching process, the grating with a Cu layer has been completely etched down to the substrate, even in grooves (figure 4.(b)). The red star in figure 2 shows that depositing the metallic layer has increased the etching speed five times compared to non-conductive photoresist coating. The grating is shown in figure 4.(b) possess the narrowest slot (width of 0.7 μm). Etching a grating with this narrow slot width with no conductive layer was not practical in this study. The charging effect is significantly severed by narrowing down the slot width. Thus etching a grating with a slot width less than 1 µm, with our optimized receipt, is practically impossible. This observation is well-matched with the theory expanded priory in this section.

4. Conclusion

This study reports an effort to etch PbSe-based submicron grating structures with the RIE method. RIE indicating high directionality is a suitable method to precisely etch small-size structures. Our previous research has studied effective parameters, including RF power, gas ratio, and process pressure in etching the smoothed edge profile. However, we noticed that by decreasing the grating size and narrowing down the slot width, a severe RIE-lag is observed. While the open area is etched completely to the substrate, the etching process is unfinished in slots, and the trench's bottom indicates a rounded shape resulting from the bowing effect.

In this research, charged shading effect and ion-focusing were suggested as responsible mechanisms causing the bowing effect. Therefore, we anticipate that introducing a thin metallic layer can neutralize the accumulated charge and address this issue and its consequent phenomena. To test this theory, a thin layer of Cu (70 nm) is deposited on the grating pattern. Comparing the etched profiles of structures with and without the Cu layer showed the effectiveness of the suggested solution. By introducing a Cu layer, we succeeded in etching a grating with a slot width of $0.7 \mu m$. However, in a case that no metallic layer is introduced, due to the severe charging effect, etching gratings with less than 1 μm slot width is impossible with our current RIE method. Therefore, we indicated that introducing a metallic layer can significantly improve the etch profile of sub-micron gratings, facilitating the fabrication of close-pitch and high-density structures with applications in enhancing the light-matter interaction.

5. Acknowledgments

The authors acknowledge the Oklahoma Center for the Advancement of Science and Technology's Research Grant #AR21-052. T.H. would like to thank the University of Oklahoma (OU) Gallogly College of Engineering for Dissertation Excellent Reward and OU Graduate College for OU Alumni Graduate Fellowship and their support.

References

- T. Hemati, B. Weng, Theoretical study of leaky-mode resonant gratings for improving the absorption efficiency of the uncooled midinfrared photodetectors, Journal of Applied Physics 124 (5) (2018) 053105.
- [2] A. Tittl, A.-K. U. Michel, M. Schäferling, X. Yin, B. Gholipour, L. Cui, M. Wuttig, T. Taubner, F. Neubrech, H. Giessen, A switchable mid-infrared plasmonic perfect absorber with multispectral thermal imaging capability, Advanced Materials 27 (31) (2015) 4597–4603.
- [3] W. Petrich, Mid-infrared and raman spectroscopy for medical diagnostics, Applied Spectroscopy Reviews 36 (2-3) (2001) 181–237.
- [4] M. Lo, C. Marcott, M. Kansiz, E. Dillon, C. Prater, Sub-micron, non-contact, super-resolution infrared microspectroscopy for microelectronics contamination and failure analyses, in: 2020 IEEE International Symposium on the Physical and Failure Analysis of Integrated Circuits (IPFA), IEEE, 2020, pp. 1–4.
- [5] M. Henini, M. Razeghi, Handbook of infrared detection technologies, Elsevier, 2002.
- [6] G. Yang, B. Weng, Reactive ion etching of pbse thin films in ch4/h2/ar plasma atmosphere, Materials Science in Semiconductor Processing 124 (2021) 105596.
- [7] T. Hemati, B. Weng, Theoretical design of coupled high contrast grating (chcg) waveguides to enhance co 2 light-absorption for gas sensing applications, Journal of Applied Physics 125 (15) (2019) 154502.
- [8] T. Hemati, X. Zhang, B. Weng, Towards a low-cost on-chip mid-ir gas sensing solution: chemical synthesis of lead-salt photonic materials, in: Smart Photonic and Optoelectronic Integrated Circuits XXII, Vol. 11284, SPIE, 2020, pp. 67–73.
- [9] C. S. Goldenstein, R. M. Spearrin, J. B. Jeffries, R. K. Hanson, Infrared laser-absorption sensing for combustion gases, Progress in Energy and Combustion Science 60 (2017) 132–176.
- [10] T. Hemati, Y. Zou, B. Weng, High-q surface light emission from active parity-time-symmetric gratings, Physical Review Applied 17 (4) (2022) 044023.
- [11] M. Sieger, B. Mizaikoff, Toward on-chip mid-infrared sensors (2016).
- [12] J. M. Mohan, K. Amreen, A. Javed, S. K. Dubey, S. Goel, Emerging trends in miniaturized and microfluidic electrochemical sensing platforms, Current Opinion in Electrochemistry (2021) 100930.
- [13] W. Wu, P. Rezai, H. Hsu, P. Selvaganapathy, Materials and methods for the microfabrication of microfluidic biomedical devices, in: Microfluidic devices for biomedical applications, Elsevier, 2013, pp. 3– 62.
- [14] D. Zhuang, J. Edgar, Wet etching of gan, aln, and sic: a review, Materials Science and Engineering: R: Reports 48 (1) (2005) 1–46.
- [15] R. J. Shul, S. J. Pearton, Handbook of advanced plasma processing techniques, Springer Science & Business Media, 2011.
- [16] M. Huff, Recent advances in reactive ion etching and applications of high-aspect-ratio microfabrication, Micromachines 12 (8) (2021) 991.
- [17] S. Tachi, K. Tsujimoto, S. Okudaira, Low-temperature reactive ion etching and microwave plasma etching of silicon, Applied physics letters 52 (8) (1988) 616–618.
- [18] T. Hemati, B. Weng, Experimental study of the size-dependent photoluminescence emission of cbd-grown pbse nanocrystals on glass, Nano Express 1 (1) (2020) 010030.
- [19] T. Okuno, A. A. Lipovskii, T. Ogawa, I. Amagai, Y. Masumoto, Strong confinement of pbse and pbs quantum dots, Journal of Luminescence

- 87 (2000) 491-493.
- [20] X. Zhang, J.-X. Shen, C. G. Van de Walle, Anomalous auger recombination in pbse, Physical Review Letters 125 (3) (2020) 037401.
- [21] T. Hemati, X. Zhang, B. Weng, A direct oriented-attachment growth of lead-chalcogenide mid-infrared nanocrystals film on amorphous substrates, Journal of Materials Chemistry C 8 (38) (2020) 13205– 13212.
- [22] T. Matsui, H. Sugimoto, T. Ohishi, Y. Abe, K. Ohtsuka, H. Ogata, Gainasp/inp lasers with etched mirrors by reactive ion etching using a mixture of ethane and hydrogen, Applied physics letters 54 (13) (1989) 1193–1194.
- [23] L. Henry, P. Granjoux, Novel process for integration of optoelectronic devices using reactive ion etching without chlorinated gas, Electronics Letters 24 (23) (1987) 1253.
- [24] T. Schwarzl, W. Heiß, G. Kocher-Oberlehner, G. Springholz, CH4/H2 Plasma Etching of IV-VI Semiconductors, na, 1999.